Nanoscale Advances

ROYAL SOCIETY OF CHEMISTRY

PAPER

View Article Online
View Journal | View Issue

Cite this: *Nanoscale Adv.*, 2025, **7**, 5377

Atomic-level characterization of crystal defects in a polycrystalline silicon-diamond structure

Yuxuan Yang,[a] Kaige Chen,[b] Xinlu Xue,[c] Tong Song,[a] Zhihao Zhao,[a] Xianghong Zhou,[a] Yang Zhang,*[ab] Rong Qin,*[c] Fei Li,[a] Xiangdong Ding,[a] Jun Sun[a] and Haijun Wu*[a]

Electronic-grade polycrystalline silicon of large size holds a crucial position in the semiconductor industry due to its extensive application prospects. This study aims to fill the gap in the atomic-level characterization of crystal defects within polycrystalline silicon. By employing focused ion beam technology for sample preparation and combining advanced scanning electron microscopy-electron backscatter diffraction technology with aberration-corrected transmission electron microscopy, we have uncovered that the silicon core of the polycrystalline silicon exhibits a single crystal structure and dense twinning within the polycrystalline matrix. These twins predominantly originate at grain boundaries and extend into the grains, forming on the {111} densely packed planes. At the atomic level, twin boundaries consist of atomically misaligned stacking faults. Moreover, we have observed atomic-scale distortions and the formation of additional stacking faults at dislocations within the twin boundaries, indicating significant atomic rearrangement. Interfaces composed of dislocations can cause twin boundaries to undergo near-vertical torsion, while coherent twin boundaries can induce slip in incoherent interfaces. Beyond being predominantly composed of dislocations, coherent twin boundaries also facilitate the formation of incoherent interfaces through transitions across the twin boundaries. These findings have critical implications for the development of polycrystalline silicon solar cells and provide a theoretical foundation for improving the quality of polycrystalline silicon.

Received 20th March 2025
Accepted 10th May 2025

DOI: 10.1039/d5na00262a

rsc.li/nanoscale-advances

Introduction

Polycrystalline silicon-based solar cells are extensively utilized due to their balanced high conversion efficiency and low production costs.[1,2] However, during the solidification growth of polycrystalline silicon, the singular temperature gradient or the latent heat released by crystal growth causes instability at the growth interface.[3] The volume changes caused by solid–liquid phase transitions result in the compression of grains against each other, generating high thermal stress and causing defect formation that can spread throughout the entire crystal.[4]

Experimentally, various studies using optical and electron microscopes have observed twinning, stacking faults, and the entanglement of dislocations within silicon crystals.[5–7] These defects significantly impair the electrical and optical performance of polycrystalline silicon, which is one of the reasons for its lower conversion efficiency compared to monocrystalline silicon.[5,8] Currently, the primary defects in the casting process of polycrystalline silicon are dislocations and twins, which are almost inevitable.[5–9] Despite continuous improvements in the fabrication technology of polycrystalline silicon, there are still numerous issues during its growth process. The real microstructural distribution of twins, stacking faults, and dislocations remains unclear, as does the relationship between dislocation nucleation and twinning. Presently, the characterization of polycrystalline silicon samples mainly focuses on macroscopic and mesoscopic scales, with rare characterization of large polycrystalline silicon blocks.[10,11] The specific structure of the interface between polycrystalline silicon and its matrix is not yet fully understood.

We have revealed that the crystal structure changes from the single-crystal silicon core to the epitaxial matrix in large-scale polysilicon samples by using the SEM-EBSD characterization method. We utilized Focused Ion Beam (FIB) technology to prepare electron microscope samples of polycrystalline silicon and employed advanced aberration-corrected transmission electron microscopy to characterize the atomic-level microstructure of polycrystalline silicon. The results reveal dense twinning within polycrystalline silicon, with most twins extending from the grain boundaries into the grains. Silicon

[a]*State Key Laboratory for Mechanical Behavior of Materials, Electronic Materials Research Laboratory (Key Lab of Education Ministry), School of Electronic and Information Engineering, Xi'an Jiaotong University, 710049, Xi'an, China. E-mail: zhangyang2020@xjtu.edu.cn; wuhaijunnavy@xjtu.edu.cn*

[b]*Instrumental Analysis Center of Xi'an Jiaotong University, Xi'an Jiaotong University, Xi'an 710049, China*

[c]*Qinghai Xince Technology Co., Ltd, Huanghe Hydropower Development Co., Ltd, 810007, Xining, China. E-mail: qinrong@spic.com.cn*

twins and stacking faults form on {111} densely packed planes, with a high propensity and density. At the atomic level, twin boundaries consist of stacking faults formed by atomic misalignments. Furthermore, atomic-level characterization has revealed that twin boundaries undergo an atomic layer twist at dislocations and decompose into a layer of stacking faults. Interfaces composed of dislocations can cause near-vertical torsion of the twin boundaries, while coherent twin boundaries can facilitate slip in incoherent interfaces. Besides being predominantly composed of dislocations, coherent twin boundaries also contribute to the formation of incoherent interfaces through transitions across the twin boundaries. Through aberration-corrected transmission electron microscopy, we have directly observed twins, stacking faults, dislocations, and interfaces. The visualization and characterization of a large number of crystal defects within polycrystalline silicon are not only significant for the development of polycrystalline silicon solar cells but also provide a theoretical basis for improving the quality of polycrystalline silicon.

Sample preparation

We utilized 8-inch electronic-grade polysilicon supplied by the New Energy Branch of the Upper Yellow River Hydropower Development Co., Ltd. The polycrystalline silicon was grown *via* directional solidification using a single-crystal silicon seed. The melt was cooled under a controlled temperature gradient to promote vertical grain growth. Initially, a long strip-shaped block of 20 mm × 5 mm × 5 mm was cut from the silicon core substrate interface of a large 12-inch polycrystalline silicon block using wire cutting, and its direction was marked. The block was manually ground on a rotating disc with silica paper. Subsequently, a polishing cloth in conjunction with a diamond polishing solution (0.15 μm) was employed for the polishing operation until the scratches were uniformly aligned under an optical microscope and the surface exhibited a mirror-like effect macroscopically. Finally, a silica polishing solution (0.05 μm) was used for polishing to achieve a matte effect. The sample was then placed in absolute ethanol and acetone successively for ultrasonic cleaning to thoroughly remove residual hydrocarbons on the polished surface. Lastly, an ion thinning instrument was used to perform surface re-polishing on the ground sample. The power was set to 3.8 kV, the tilt angle was set to 15°, and the duration was from 15 minutes to 30 minutes (Fig. 1(a)). After the polishing treatment, the sample met the full-scale observation requirements from the macroscopic scale to the mesoscopic scale and then to the microscopic scale. Subsequently, a scanning electron microscope (SEM) equipped with electron backscatter diffraction (EBSD) was employed to conduct microscopic observation and orientation characterization of the material (Fig. 1b–b2).

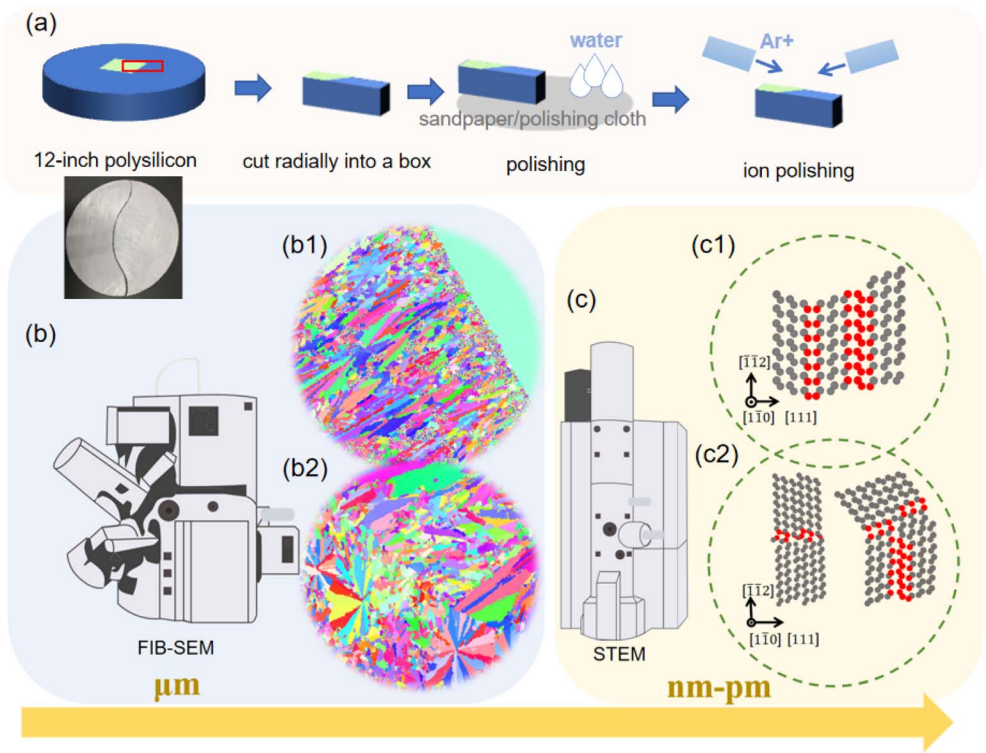

Fig. 1 Flow chart of polysilicon bulk sample preparation; (a) flow chart of polysilicon bulk polishing; (b–b2) schematic diagram of SEM-EBSD characterization; (c–c2) schematic diagram of STEM characterization; this polysilicon is composed of a silicon core and its surrounding matrix, as depicted in (a), with the core being monocrystalline and the matrix being polycrystalline. We utilized a Thermo Scientific Helios 5 UX focused ion beam (FIB) microscope to extract and thin samples at the interface between the polysilicon core and its matrix (the sampling location is represented with the red square in Fig. 3a). The samples prepared *via* the FIB were then examined using a JEM-ARM300F2 aberration-corrected electron microscope (c–c2).

Results

1. Polycrystalline silicon interface morphology

With the observations made by SEM-EBSD, we have generally established an understanding of the grain morphology and its evolution patterns from the core to the surface of the polysilicon wafer. SEM-EBSD was performed on the silicon core, interface, substrate, and near surface of polycrystalline silicon. The shooting locations are marked as e, f, g, and h in Fig. 2(a), and FIB samples were taken at the interface between the silicon core and substrate for STEM, as shown in Fig. 2(b–d). The silicon core of polysilicon exhibits a typical single-crystal structure, with large-scale twins present inside, as shown in Fig. 2e–e1. In the large-scale epitaxial growth of polysilicon, the single-crystal silicon core provides a starting point for the formation of polysilicon. The region adjacent to the interface serves as a small-grain nucleation zone. Near the nucleation zone, dendrite-like columnar crystals approximately 400 μm thick are observed, extending outward perpendicular to the interface, forming a significant contrast with other matrix regions, as shown in Fig. 2f–f1.

The matrix region far from the interface features a crystal structure with a radial pattern morphology, having no specific orientation. The grain size is around 10–20 μm, as shown in Fig. 2g–h1. The formation of the radial-pattern crystals is attributed to the relatively high solidification rate at a lower temperature in this region, resulting in a fast nucleation and growth rate. The reduction in the orderliness degree of the polycrystalline regions directly leads to the deterioration of electrical properties, resulting in a lower breakdown voltage and limited applications. In addition, the presence of various grain regions leads to an increase in defects, which is unfavorable for the large-scale epitaxial growth of polycrystalline silicon.

SEM-EDS analysis at the interface reveals the enrichment of oxygen, as shown in Fig. 2i. Because we used 11N electron grade polycrystalline silicon as the sample, it can be seen that the sample contains almost no impurities such as carbon and phosphorus, and only a small amount of oxygen enrichment is observed at the interface. The oxygen impurities in the ingot are mainly introduced in the form of SiO gas, and SiO has two sources:[12,13] (1) the reaction between the melt and the quartz crucible (mainly composed of SiO_2) at high temperature: SiO_2+Si → SiO; (2) the graphite heater reacts with the quartz crucible to generate SiO. Some of the SiO generated in the ingot furnace evaporates from the surface of the melt, while the remaining part dissolves into the melt SiO → Si + O, thereby introducing oxygen impurities.

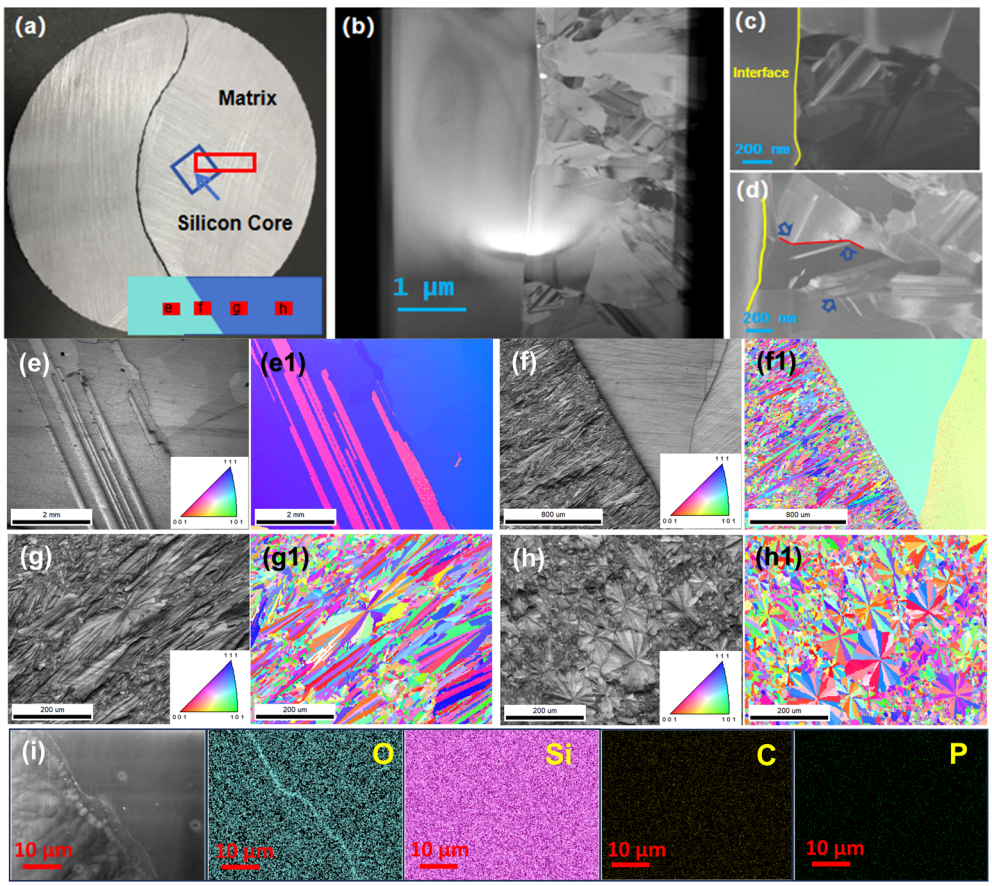

Fig. 2 (a–d) The twin structures within the polycrystalline silicon matrix, as observed under an aberration-corrected electron microscope; (e–e1) SEM-EBSD images of the polysilicon core; (f–f1) SEM-EBSD of the polysilicon interface; (g–h1) SEM-EBSD EBSD of the polysilicon matrix; (i) SEM-EDS image of the polysilicon interface.

The enrichment of oxygen impurities directly affects the deposition and growth of subsequent crystals, accelerates the grain nucleation rate in the early stage of deposition, and easily exacerbates the formation of defects such as twin dislocations. The enrichment of oxygen impurities at the interface may be one of the critical factors restricting the growth of large-scale polysilicon.

2. Twin structures in silicon

Preliminary imaging of the prepared samples was conducted using a scanning transmission electron microscopy (STEM) probe equipped on the FIB, as illustrated in Fig. 2b–d. The silicon core is characterized by a typical single-crystal structure, exhibiting a smooth and uniform surface without any minor dendrites. Within the matrix, a polycrystalline structure is clearly observable, with densely packed, fine twins that are parallel to each other. These twins extend from the grain boundaries into the interior of the crystal (in Fig. 2d, the red lines represent the grain boundaries and the blue arrows point to the twins). During polysilicon solidification, mutual compression between adjacent grains generates localized high stress. This stress concentration facilitates twin nucleation preferentially at grain boundaries (GBs), followed by propagation into the grain interior.

Dense twins and stacking faults can be observed within the grains of the polycrystalline silicon matrix. In Fig. 3b and c, the blue square encloses a stacking fault, while the red lines indicate the boundaries of twins.

The silicon crystal adopts a diamond cubic structure, which can be viewed as two interpenetrating face-centered cubic (FCC) lattices offset by 1/4 of the body diagonal. Besides the typical FCC arrangement, there are four additional atoms within the cube, positioned at the centers of four of the tetrahedral voids in the crystal. The normal stacking order along the [111] direction for a face-centered cubic crystal is ABCABCABC. However, for silicon crystals along the [111] direction, the structure is composed of a/a″, b/b″, and c/c″ forming three double layers as a repeating unit, as illustrated in Fig. 3(d and f), which show schematic diagrams of the common diamond structure. As shown in the left image in Fig. 3g, within the [111] direction's double layers, layer a″ is covered by layer b and layer b″ is covered by layer a. This arrangement directly leads to the occurrence of stacking faults in silicon crystals, where the front view of the (111) plane shows the superposition of two double layers, as depicted in the right image in Fig. 3g.

Fig. 3(e) shows a schematic diagram of the formation of coherent twin boundaries in the silicon crystal along the [110] direction, where the double layers are collectively referred to as a, b, and c. When twinning occurs, the atomic arrangement transforms into a symmetric relationship, changing from abcabc to abcc′b′a′. This principle is similar to the formation of twins in Cu and Al, with the distinction being the unique double-layer atomic structure of the silicon (111) plane.

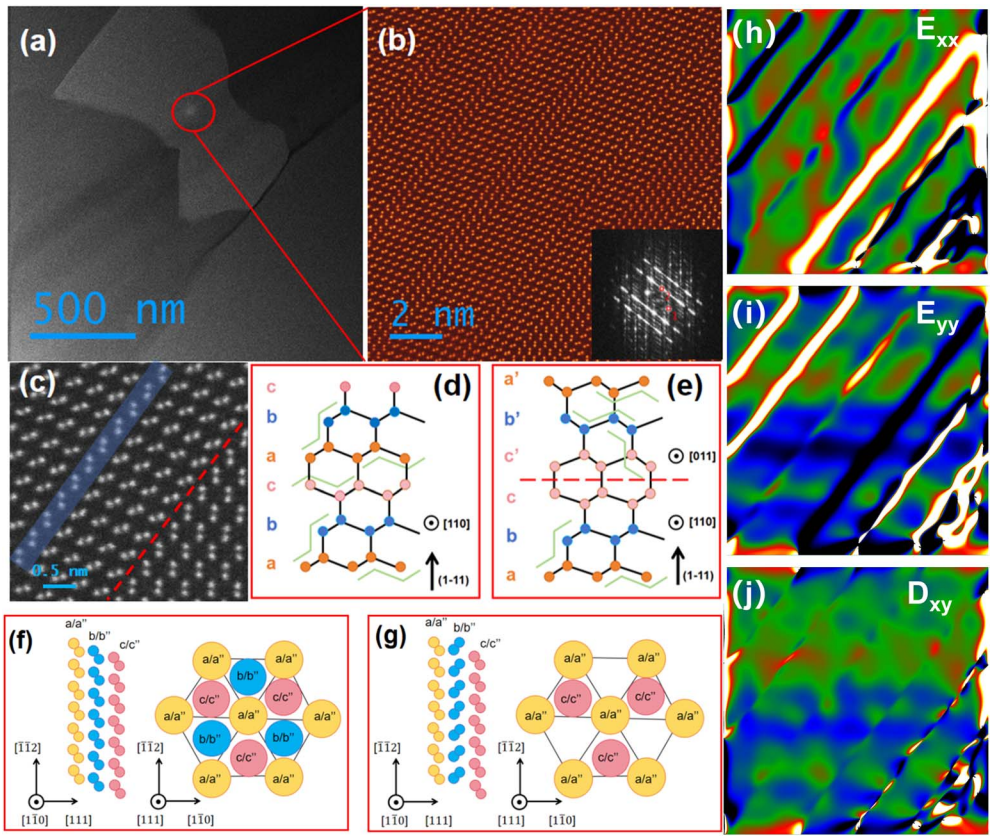

Fig. 3 (a–c) HADDF images of the silicon stacking faults and twinning. (d–g) Schematic diagrams of the twin structures in the silicon crystal. (h–j) Local stress analysis diagrams of (b).

The formation of twins is generally considered a nucleation and growth process, where twinning nucleation occurs at sites of localized high stress concentration, then expands and eventually covers the entire grain.[11,14,15] We conducted a detailed local stress analysis of Fig. 3b, as shown in Fig. 3(h–j), and observed significant axial stress in the x and y directions, with almost no shear stress. It can be inferred that the occurrence of dense twinning within the grain is caused by tensile stress and tensile stress in the x and y directions, rather than shear stress.

3. Kinking and termination of twins in silicon

Using an aberration-corrected electron microscope to further characterize the twin structures in polycrystalline silicon, as shown in Fig. 4(a–e), it is evident that the twin boundaries within the polysilicon grains have undergone various degrees of twisting. The red lines in the images represent coherent twin boundaries, where the twinning plane and the twin boundary coincide, while the yellow squares indicate incoherent twin boundaries, and the yellow vertical symbols represent dislocation structures.

As seen in Fig. 4(b), the formation of dislocation defects somewhat impedes the extension of the twin boundary. Where there were originally five layers of atoms between two twin boundaries, the formation of a dislocation defect reduces this to four layers of atoms and results in the segregation of a stacking fault. As illustrated in Fig. 4(c), the formation of incoherent twins also causes twisting of the twin boundary. However, unlike coherent boundaries, incoherent boundaries are to some extent composed of dislocations. Notably, the longer 14-layer twin boundary twist in Fig. 4(c) does not induce the appearance of a stacking fault, whereas the twists in layers 1 and 4 in Fig. 4(a) and (c) both induce the appearance of a stacking fault. Moreover, incoherent boundaries are mostly perpendicular to the coherent twinning planes, causing the twins to undergo nearly vertical twists.

As shown in Fig. 4e, incoherent interfaces, mostly composed of dislocations, appear bent and uneven. However, a peculiar phenomenon observed at incoherent interfaces is the nearly horizontal slippage caused by coherent twin boundaries. The presence of coherent twin boundaries, represented by red straight lines in Fig. 4e, induces slippage in the incoherent interfaces. Additionally, the presence of microcoherent twins on the incoherent twin boundaries is observed, mostly two atomic layers wide and symmetric about the twin, with lengths of 2–3 atomic layers. The presence of these coherent twin boundaries connects the incoherent interfaces, reducing stress concentration at the interface to some extent. As shown in Fig. 4(h–j), the stress concentration is significantly reduced at the non-coherent interface, and the stress distribution is flat and uniform without obvious red and dark blue stress concentration areas. The formation of twins is mainly due to the compressive stresses in the x and y directions during the solidification process, rather than the shear stress, as shown in Fig. 4(h–j).

Currently, in the casting process of polycrystalline silicon, the main defects are dislocations and twins, which are always challenging to avoid. The impact of dislocations on the crystal's

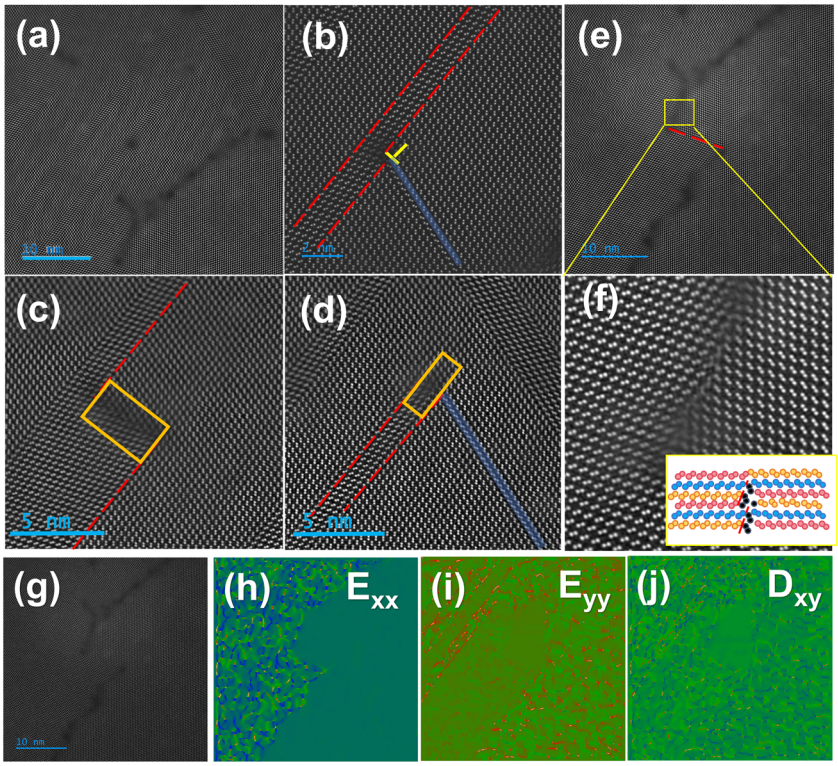

Fig. 4 (a–g) HADDF images of twins kinking and termination twins in silicon (red straight lines indicate coherent twin boundaries along {111} planes, while yellow curves represent incoherent boundaries/dislocations); (h–j) local stress analysis diagrams of (g).

performance is primarily manifested in the following aspects:[14–16] for silicon materials, the higher stress around dislocation lines causes lattice distortion, changing the structure of central atomic bonds and introducing a large number of electrically active centers, forming new energy band structures between the conduction band and the valence band; dislocation lines can become recombination centers for non-equilibrium carriers, thus promoting the recombination annihilation of non-equilibrium carriers and reducing the lifetime of minority carriers; dislocations can serve as transport channels for electrons or diffusion pathways for atoms, affecting the crystal's resistivity or diffusion coefficient.

During the crystal growth process, twins occupy more than 60% of the total interface area of polycrystalline silicon,[6] which also affects the crystal's performance. We found that there exists a certain correlation between dislocation nucleation and twin boundaries, where the presence of twin boundaries can induce the generation of dislocations. Twin boundaries can prevent the slip of dislocations, leading to the accumulation of dislocations in front of the twin boundaries, increasing dislocation density, and simultaneously increasing the crystal's resistance to plastic deformation.[16–18] Due to changes in bonding characteristics, the absorption of light and carrier properties near the twin boundaries will change.[18,19] The kinking and termination of twins release, to a certain extent, the internal stress formed during the solidification process, as shown in Fig. 4(g–j).

Conclusion

This study provides a comprehensive atomic-level analysis of crystal defects in polycrystalline silicon, significantly advancing our understanding of its internal structure. The characterization of twins, stacking faults, and dislocations reveals intricate details about the defect formation mechanisms and their implications for the material's properties. These insights are invaluable for improving the performance and quality of polycrystalline silicon, particularly in solar cell applications. By elucidating the atomic-scale interactions and transformations within polycrystalline silicon, this research paves the way for targeted improvements in manufacturing processes and material quality, ultimately contributing to the development of more efficient and reliable polycrystalline silicon-based technologies.

Data availability

All relevant data.

Conflicts of interest

There are no conflicts to declare.

Acknowledgements

The authors would like to acknowledge the financial support from the National Key R&D Program of China (2021YFB3201100), the National Natural Science Foundation of China (52172128 and 52472250), and the Top Young Talents Programme of Xi'an Jiaotong University. The authors would like to acknowledge the strong support from the Instrumental Analysis Center of Xi'an Jiaotong University, with special thanks to Chuansheng Ma for his support in aberration-corrected STEM.

References

1 F. Zhang, S. Rao, F. Wang, *et al.*, Research Progress on the Solid-liquid Interface in the Crystal Growth of Polycrystalline Silicon, *J. Synth. Cryst.*, 2017, **46**(10), 2077–2082.
2 H. Jiang, Analysis on the development of electronic grade polysilicon in China, *Sci. Technol. China*, 2021, **04**, 64–66.
3 B. Ryningen, G. Stokkan, M. Kivambe, *et al.*, Growth of dislocation clusters during directional solidification of multicrystalline silicon ingots, *Acta Mater.*, 2011, **59**(20), 7703–7710.
4 A. Jouini, D. Ponthenier, H. Lignier, *et al.*, Improved multicrystalline silicon ingot crystal quality through seed growth for high efficiency solar cells, *Prog. Photovoltaics*, 2012, **20**(6), 735–746.
5 K. Kutsukake, T. Abe, N. Usami, *et al.*, Generation mechanism of dislocations and their clusters in multicrystalline silicon during two-dimensional growth, *J. Appl. Phys.*, 2011, **110**(8), 083530.
6 A. Voigt, E. Wolf and H. P. Strunk, Grain orientation and grain boundaries in cast multicrystalline silicon, *Mater. Sci. Eng., B*, 1998, **54**(3), 202–206.
7 K. Nakai, M. Hasebe, K. Ohta, *et al.*, Characterization of grown-in stacking faults and dislocations in CZ-Si crystals by bright field IR laser interferometer, *J. Cryst. Growth*, 2000, **210**(1), 20–25.
8 L. V. C. Assali, Electrically active centers in partial dislocations in semiconductors, *Phys. B*, 2001, **308**, 489–492.
9 Q. Chen, X. Y. Liu and S. B. Biner, Solute and dislocation junction interactions, *Acta Mater.*, 2008, **56**(13), 2937–2947.
10 G. Stokkan, Twinning in multicrystalline silicon for solar cells, *J. Cryst. Growth*, 2013, **384**, 107–113.
11 K. Fujiwara, K. Maeda, N. Usami, *et al.*, Formation mechanism of parallel twins related to Si-facetted dendrite growth, *Scr. Mater.*, 2007, **57**(2), 81–84.
12 Y. Xingping, G. Lijie, L. Qinghui, *et al.*, Product quality research in the industrialized preparation of electronic grade polysilicon: a review of impurity sources and control strategies, *Renewable Sustainable Energy Rev.*, 2025, **214**, 115569.
13 B. Domeij and A. Diószegi, The Distribution of Carbon in Austenite Studied on a Water-Quenched Compacted Graphite Iron Using Electron Probe Microanalysis, *Int. J. Metalcast.*, 2020, **14**(3), 782–793.
14 A. Fedotov, A. Mazanik and A. Ulyashin, Electrical activity of grain boundaries in silicon bicrystals and its modification by hydrogen plasma treatment, *Sol. Energy Mater. Sol. Cells*, 2002, **72**(1–4), 589–595.
15 X. Quan, N. Yuan, J. Ding, *et al.*, Growth of multicrystalline silicon assisted by electrophoretic deposited quartz[J/OL], *Sol. Energy*, 2021, 797–802.

16 L. Wang, H. Liu and X. Liu, Electron Radiation Effects of Grain-Boundary Evolution on Polycrystalline Silicon in MEMS[J/OL], *Micromachines*, 2022, 743.
17 A. Richter, R. Müller, B. Jan, *et al.*, Design rules for high-efficiency both-sides-contacted silicon solar cells with balanced charge carrier transport and recombination losses, *Nat. Energy*, 2021, **6**(4), 429–438.
18 Q. Kang, *et al.*, Thermal cycle impact on polycrystalline silicon: direct observation of electrical properties degradation and interfacial nanocrystalline grain defects, *Nano Res.*, 2025, **18**(6), 94907398.
19 C. Zhang, Y. R. Luo, K. Li, *et al.*, The influence of a threading dislocation on (110) interface morphology and growth rate of silicon crystal growth from melt, *Appl. Phys. A:Mater. Sci. Process.*, 2016, **122**(11), 954.